ISSN 1063-7710, Acoustical Physics, 2019, Vol. 65, No. 2, pp. 171–177. © Pleiades Publishing, Ltd., 2019.

PHYSICAL ACOUSTICS

Acoustic Wave Propagation Along Piezoelectric Plate Coated with Piezoelectric Films[1]

V. I. Anisimkin[a], *, E. Verona[a, b], A. S. Kuznetsova[a], and V. A. Osipenko[c]

[a] *V.A. Kotel'nikov Institute of Radio Engineering and Electronic, Russian Academy of Sciences, Moscow, 125009 Russia*

[b] *Institute for Photonics and Nanotechnologies, Italian National Research Council (IFN-CNR), Roma, I-00156 Italy*

[c] *Acoustoelectronics and Piezoceramic Elpa Corporation, Zelenograd, Moscow, 124460 Russia*

**e-mail: anis@cplire.ru*

Received June 18, 2018; revised August 30, 2018; accepted October 30, 2018

Abstract—A novel solid state structure consisting of piezoelectric plate sandwiched between two piezoelectric films is suggested as propagation medium for acoustic waves. Considering, as an example, quartz plate coated with AlN film and with AlN film together with ZnO film, the main characteristics of the Lamb and SH acoustic modes are numerically calculated and compared with each other. It is shown that i) the range of acoustic parameters achievable in structures is wider than that is for an uncoated plate, ii) generation of waves in the plate with one film is accomplished by 12 transducer configurations, while there are 32 configurations to excite the same waves in two film structure, iii) dispersion of the wave velocities and coupling constants depend on the mode order, mode type, film thickness, plate thickness, and transducer configuration. This property makes selection of appropriate modes more flexible. Results of calculations are partially verified experimentally.

Keywords: piezoelectric plate, piezoelectric film, acoustic modes, velocity, coupling constant, displacements

DOI: 10.1134/S1063771019020027

1. INTRODUCTION

Acoustic wave propagation has already been studied for many solid state structures – infinite substrates ($-\infty < H < +\infty$), semi-infinite substrates ($-\infty < H < 0$), film/substrate material combinations ($h \ll \lambda$, $-\infty < H < 0$), uncoated plates ($h = 0$, $H \sim \lambda$), etc. As a result, different BAWs, SAWs, pseudo-SAWs, plate modes, and some other waves have been found in such media [1–6]. On the other hand, the same study for the plates ($H \sim \lambda$) coated with thin films ($h \ll \lambda$) has been accomplished only for Al film/AlN plate, ZnO film/Si plate, and ZnO film/Si plate/ZnO film material combinations [7–12]. At the same time, new geometries and material combinations with various acoustic and piezoelectric properties may offer other properties and phenomena. For example, deposition of the film of one piezoelectric material on the plate of the other material may be used for precise tuning of the operation frequency of filters, resonators, delay lines, sensors, and other acousto-electronic devices. Using appropriate transducer configuration may provide better electromechanical transduction for desirable mode generation. Combination of the transducer configuration with mode order, film thickness, and plate thickness may ensure rejection of unwanted modes in the stop-band of the devices. Trapping the mode energy to the plate surface may be used for increasing sensitivity of the mode towards electrical and mechanical loadings.

The goal of the present paper is twofold: first, to study acoustic wave propagation along new media consisting of piezoelectric plate and piezoelectric films; second – to compare characteristics of waves of the same type in the coated and uncoated plates of the same material.

2. STRATEGY

As an example, the properties of waves were studied for uncoated ST-quartz plates with two mutually orthogonal propagation directions on one wafer (Eugler angles 0°, 132.75°, 0° and 0°, 132.75°, 90°) and for the same plate coated with single AlN film (0°, 0, 0°) or sandwiched between AlN and ZnO films (0°, 0, 0°). The plate thickness H normalized to the acoustic wavelength λ was taken as $H/\lambda = 1.67$. The thicknesses of the films were changed in the ranges $0 \le h_{AlN}/\lambda \le 0.1$ and $0 \le h_{ZnO}/\lambda \le 0.2$, respectively.

The choice of materials was suggested by their world-wide distribution and large difference in acoustic and piezoelectric properties. For instance, on considering the Rayleigh wave propagation, the phase

[1] The article is published in the original.

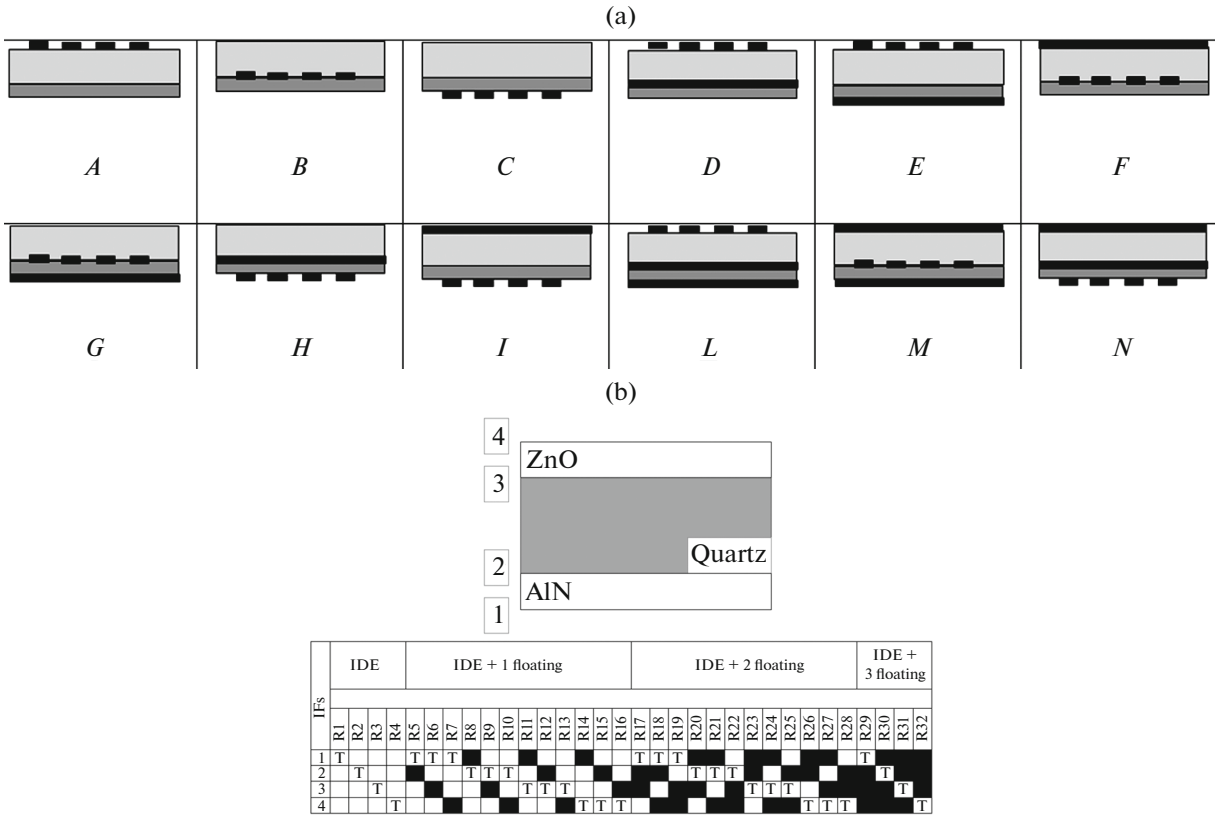

Fig. 1. Transducer configurations for piezoelectric plate coated with (a) one and (b) two piezoelectric films. 1, 2, 3, 4 – interfaces (IFs); T – interdigital electrodes (IDEs); ■ – floating electrode.

velocities V in AlN, SiO_2, and ZnO are respectively of 5607, 3158, and 2680 m/s, while the corresponding electromechanical coupling coefficients K^2 are 0.28, 0.11, and 0.98%. So that, as compared with quartz, AlN may be considered as "fast and piezoelectrically close" material, while ZnO as "slow and piezoelectrically strong" material.

Numerical calculations of the phase velocity $V(h/\lambda)$ and electromechanical coupling constant $K^2(h/\lambda)$, as well as the longitudinal $U_1(x_3/\lambda)$, shear horizontal $U_2(x_3/\lambda)$, and shear vertical $U_3(x_3/\lambda)$ displacements of the Lamb waves propagating in the uncoated and coated plates were accomplished using the well-approved software [13], together with the material constants of Ref. [14]; following the procedure described in details in Refs. [8, 9]. Independent non-zero material constants used in calculations are as follows.

1. For hexagonal ZnO.

—elastic constants (in 10^{11} N/m^2): $c_{11} = 2.09$, $c_{12} = 1.205$, $c_{13} = 1.046$, $c_{22} = 2.096$, $c_{33} = 2.106$, $c_{44} = 0.423$, $c_{66} = 0.4455$; piezoelectric constants (in 10^{-11}F/m): $e_{15} = -0.48$, $e_{31} = -0.573$, $e_{33} = 1.321$; dielectric constants (in C/m^2): $\varepsilon_{11} = 7.57$, $\varepsilon_{33} = 9.03$; density (in 10^3 kg/m^3): $\rho = 5.665$.

2. For hexagonal AlN.

—elastic constants (in 10^{11} N/m^2): $c_{11} = 3.45$, $c_{12} = 1.25$, $c_{13} = 1.2$, $c_{22} = 3.45$, $c_{33} = 3.95$, $c_{44} = 1.18$, $c_{66} = 1.1$; piezoelectric constants (in 10^{-11} F/m): $e_{15} = -0.48$, $e_{31} = -0.58$, $e_{33} = 1.55$; dielectric constants (in C/m^2): $\varepsilon_{11} = 8.0$, $\varepsilon_{33} = 9.5$; density (in 10^3 kg/m^3): $\rho = 3.26$.

The electromechanical coupling coefficients K^2 in the AlN/quartz bi-layered structure were considered for twelve configurations shown on Fig. 1a. The same coefficients in AlN/quartz/ZnO triple-layered structure were considered for thirty-two different transducer configurations shown on Fig. 1b. These configurations are distinguished of each other by location of interdigital and floating electrodes (if any) at the four interfaces (IF) indicated as 1, 2, 3, and 4 on Fig. 1b. Note, for the same bi-layered structure with piezoelectric layer and non-piezoelectric plate, the number of different transducer configurations is only four [8, 9].

Results of calculations were experimentally verified using acoustic delay lines implemented on ST-quartz plate ($H = 500$ μm) with two pairs of interdigital electrodes aligned along the X-axis and perpendicular to the axis in order to generate the Lamb and SH-modes, respectively. Each transducer consisted of 20 finger electrodes patterned from Cr/Al, 1000 nm thick.

Table 1. Properties of the Lamb modes in coated ST,X-quartz plates referred to the uncoated counterpart: $H/\lambda = 1.67$, $h_{AlN}/\lambda = 0...0.01$, $h_{ZnO}/\lambda = 0...0.02$

n	Parameter	Quartz plate	AlN/quartz plate	AlN/quartz plate/ZnO
1	V, m/s K^2, %	3045 0.078 (IDE + floating)	3045–3125 (+2.6%) 0–0.105 (+35%)	3125–2868 (–8%) 0–0.736 (+843%)
2	V, m/s K^2, %	3482 0.063 (IDE + floating)	3482–3593 (+3.2%) 0–0.148 (+135%)	3593–3425 (–4.7%) 0–0.222 (+252%)
3	V K^2, %	4889 0.00115 (IDE + floating)	4815–4905 (**–1.5**...+0.33%) 0–0.054 (+4596%)	4905–3433 (–29%) 0–0.225 (+19465%)
4	V, m/s K^2, %	5111 0.018 (IDE without floating)	5101–5112 (**–0.2**...+0.02%) 0–0.0385 (+115%)	5112–4410 (–13.7%) 0–0.475% (+1134%)

Period of the transducers and the distance between them were $\lambda = 300$ μm and $L = 16.5$ mm, respectively. In our tests we preferred the more technologically simple configuration R3 (Fig. 1) with interdigital electrodes every time on the surface 3 allowing operation both with coated and uncoated plates. The frequencies of waves were in the range 10–40 MHz.

The technology of the films fabrication accounted for the difference in the expansion coefficients of the AlN, quartz, and ZnO materials.

The *c*-oriented textured AlN films were fabricated on the surface 2 (Fig. 1b) in magnetron sputtering system using 50% Ar + 50% N_2 gas mixture, 0.1 Pa gas pressure, and Al target (99.999%) 140 mm in diameter. The distance between target and substrate was 70 mm, and the discharge power was 800 W. The sputtering rate and the thickness of the film were 0.7–0.8 μm/h and 3 μm ($h_{AlN}/\lambda = 0.1$), respectively. The substrate temperature was 150°C.

The fabrication of the *c*-oriented textured ZnO films on the surface 3 (Fig. 1b) was performed in triode sputtering system with dc current using ZnO target, 80% Ar + 20% O_2 gas mixture, and 0.07 Pa pressure. The substrate temperature was 200°C, the rate of the sputtering was 1.2–3 μm/h, and the thickness of the film was 3.2 μm ($h_{ZnO}/\lambda = 0.107$).

For configuration R3 of interdigital electrodes (Fig. 1) used in experiments the ZnO and AlN films were deposited both on free and periodically metalized surfaces of the quartz substrates. The X-ray analysis of the films in these two regions demonstrated that the film difference existed only in very thin initial layers (0.1 μm thick), which were very small as compared with total thickness of the films (3 μm). Therefore, the films may be considered as homogeneous along the whole propagation path from input to output transducer.

The test delay lines were tested by the network analyser (Keysight E5061B) operating in amplitude format. The measured parameters were i) the change in the phase velocities produced by the presence of the films ($\Delta V = \Delta f\lambda$, where f is the mode frequency and λ is the transducer period), ii) the attenuation of modes due to the film deposition, and iii) the attenuation of modes produced by viscous liquid (glycerin) whose value is proportional to the mode displacements U_1, U_2, and U_3 on the top and bottom faces of the structures. Details of the measurements are presented elsewhere [5, 8, 9].

3. RESULTS AND DISCUSSION

Results of calculations are shown on Figs. 2–4 and in Tables 1, 2.

Figure 2 presents dispersion of modes in the AlN/quartz bi-layered structure. It turns out that velocities V of all modes are almost independent on transducer configuration, but they are varied with the film thickness h_{AlN}/λ differently. In particular, for any h_{AlN}/λ the film accelerates first two Lamb modes ($n = 1, 2$) and first three SH-modes ($n = 1, 2, 3$), but it slows down other modes in contrast with Rayleigh wave propagation in layered structure with "fast" on "slow" material combination [15].

At the same time, the coupling coefficients K^2 of modes depend on transducer configurations strongly (Fig. 2c). For example, for configuration A (Fig. 1a) and modes $n = 1, 4$ curves $K^2(h/\lambda)$ are every time increased with h_{AlN}/λ, while for configuration N (Fig. 1a) and modes $n = 2, 3$ curves are increased for $h_{AlN}/\lambda < 0.03$ and decreased for $h_{AlN}/\lambda > 0.03$. Therefore, for thick AlN films, when $K^2 = 0$, these modes are not excited.

Curves $V(h/\lambda)$ and $K^2(h/\lambda)$ for the AlN/quartz/ZnO structure demonstrate similar behavior (Fig. 3): velocities of modes do not depend on transducer configuration, while the coupling coefficients $K^2(h/\lambda)$ do; for some modes, transducer configuration, and ZnO thickness the coefficients K^2 approach large values 0.3–0.8%. Moreover, as ZnO material is much "slower" as compared with AlN and quartz, it decreases velocities of all modes at any thickness.

Once the surface of the plate is covered with one or two layers of different thickness and materials, the propagation of the Lamb and SH- modes is modified

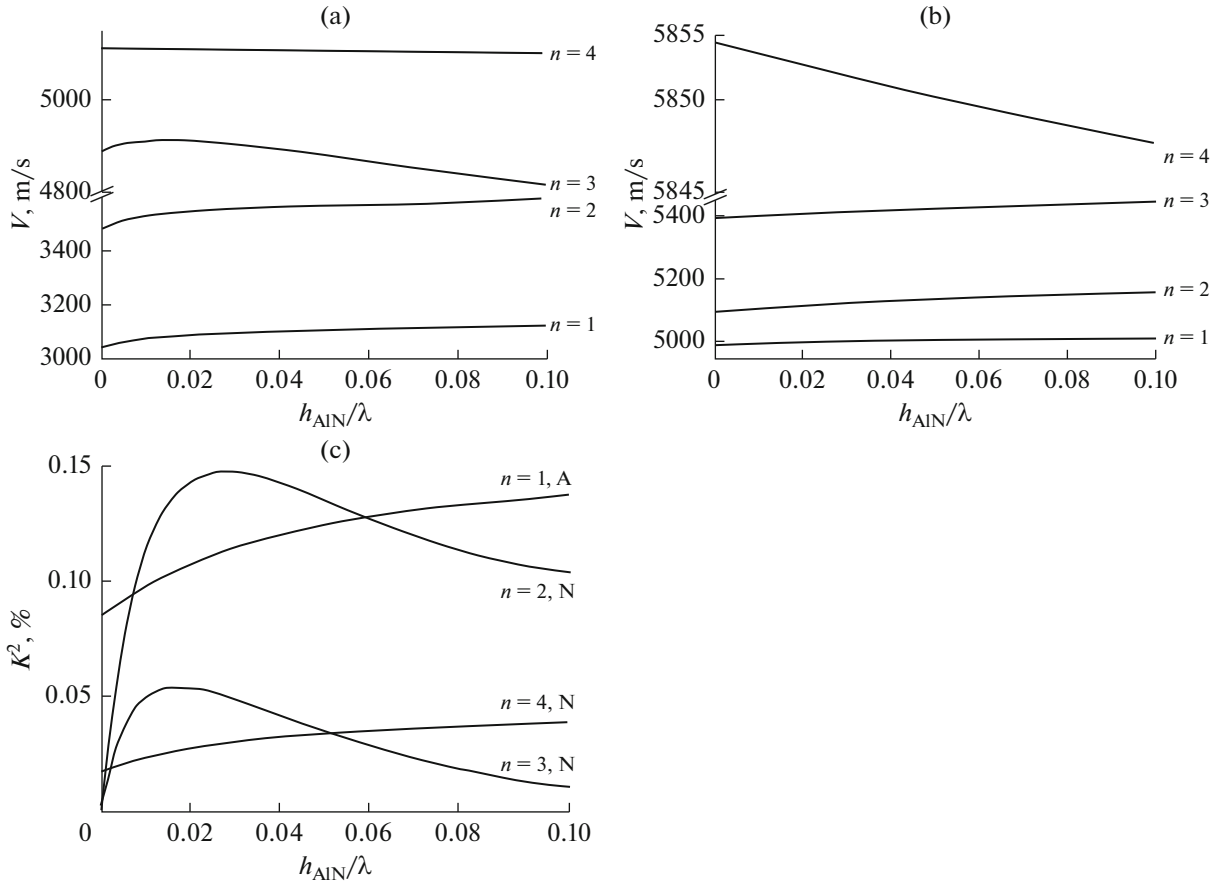

Fig. 2. Dispersion of acoustic waves in the AlN film/quartz plate layered structure. (a) Lamb modes, ST,X-quartz plate, $H/\lambda = 1.67$; (b) SH-modes, ST,X+90°-quartz plate, $H/\lambda = 1.67$; (c) Lamb and SH-modes for particular transducer configurations according to Fig. 1.

not only in the phase velocities and coupling constants, but in amplitude profile as well. For example, for zero Lamb mode in the AlN/quartz structure, the surface displacements on the interfaces 1 and 3 (Fig. 1b) are $U_1 = 1$ and 1.7, $U_2 = 0.21$ and 0.27, and $U_3 = 1.9$ and 2.4, respectively (Fig. 4). So that, pure symmetric and pure anti-symmetric modes do not exist in coated plates, in general.

Tables 1 and 2 summarize results of calculations and compare the ranges of the acoustic parameters achievable in coated and uncoated plates. The data demonstrate that deposition of AlN and ZnO films on quartz plate allows monitoring the mode velocities V within −33...+3.2% (e.g. from 4992 to 3350 m/s or from 3482 to 3593 m/s) and the coupling constants K^2 within −78...+4596% (e.g. from 0.136 to 0.03% or

Table 2. Properties of the Lamb modes in coated ST,X + 90°-quartz plates referred to the uncoated counterpart: $H/\lambda = 1.67$, $h_{AlN}/\lambda = 0...0.01$, $h_{ZnO}/\lambda = 0...0.02$

n	Parameter	Quartz plate	AlN/quartz plate	AlN/quartz plate/ZnO
1	V, m/s	4992	4992–5011 (+0.38%)	5011–3350 (−33%)
	K^2, %	0.085 (IDE)	0–0.138 (+62%)	0–0.27 (+218%)
2	V, m/s	5096	5096–5160 (+1.25%)	5160–5065 (−1.8%)
	K^2, %	0.136 (IDE + floating)	0–0.1 (−26%)	0–0.03 **(−78%)**
3	V	5393	5393–5442 (+0.91%)	5442–5275 (−3.1%)
	K^2, %	0.0778 (IDE + floating)	0–0.06 **(−23%)**	0–0.05 **(−36%)**
4	V, m/s	5854	5854–5848 **(−0.105%)**	5848–5600 (−4.25%)
	K^2, %	0.0407 (IDE + floating)	0–0.036 (−11.3%)	0–0.03 **(−26%)**

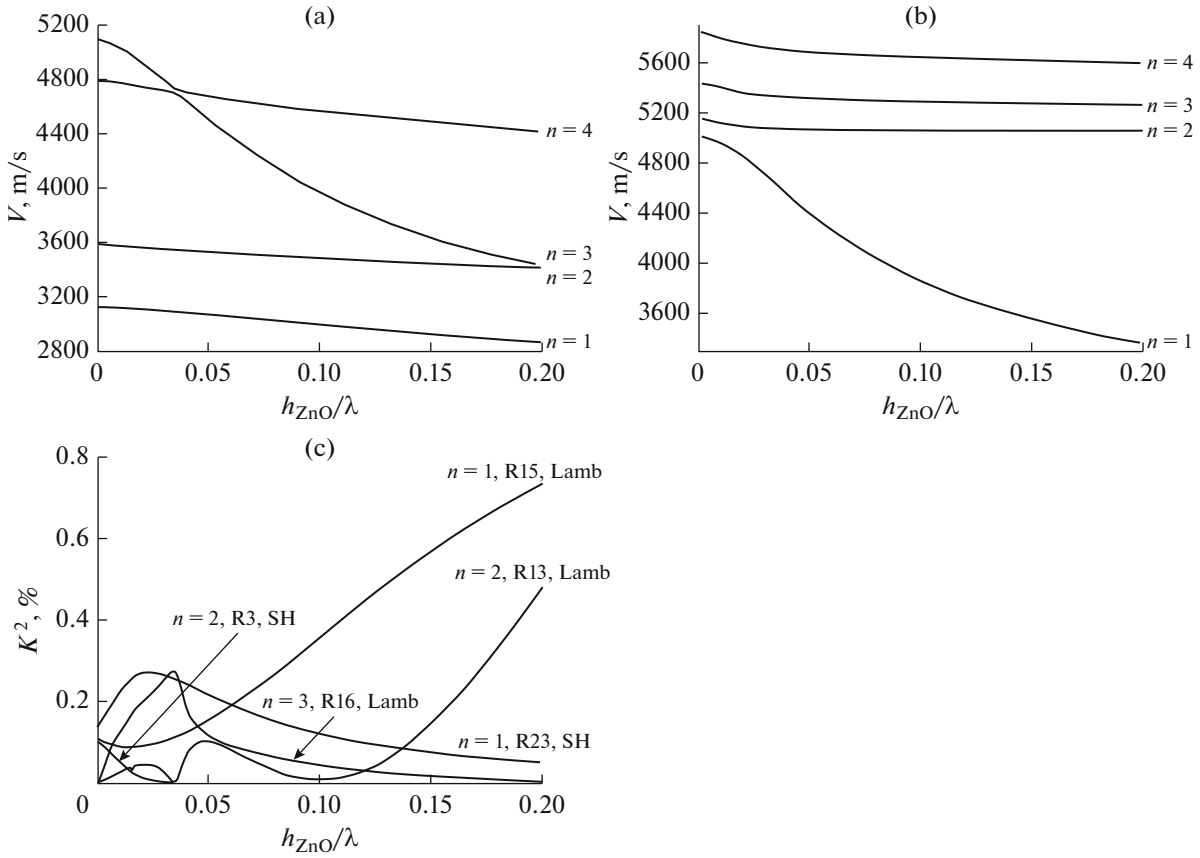

Fig. 3. Dispersion of acoustic waves in the AlN film/quartz plate/ZnO film layered structure. (a) Lamb modes, ST,X-quartz plate, $H/\lambda = 1.67$, $h_{AlN}/\lambda = 0.01$; (b) SH-modes, ST,X+90°-quartz plate, $H/\lambda = 1.67$, $h_{AlN}/\lambda = 0.01$; (c) Lamb and SH-modes for particular transducer configurations according to Fig. 1.

from 0.00115 to 0.054%) of the values V and K^2 for uncoated plate. Efficiency of the monitoring depends on the mode order, mode type, transducer configuration, and film thickness. Just as for Rayleigh waves [15], "fast" AlN film in most cases increase the mode velocities and "piezoelectrically strong" ZnO film enlarge the coupling constants. However, in contrast to Rayleigh waves [15], the properties of the mode in some cases are uncommon: the AlN film may decrease velocities of some modes (bold) and ZnO film may reduce the coupling coefficients of others (bold). These properties are inherent only for waves propagating in plates coated with piezoelectric films, but not for surface acoustic wave in the same structure.

Results of calculations are partially verified experimentally.

Figure 5a shows effect of the AlN film deposition on the mode velocities compared with relevant values in uncoated quartz plate. According to calculations (Fig. 2b), "fast" AlN film accelerates the first three SH-modes ($\Delta V/V_0 > 0$), but slows down all other counterparts ($\Delta V/V_0 < 0$). For $H/\lambda = 1.67$ and $h_{AlN}/\lambda = 0.01$ the range of the velocity variations is $-1...+0.2\%$.

Figure 5b shows the same effect for the plate sandwiched between AlN and ZnO films. Here, in accordance with calculations (Fig. 3b), velocities of all

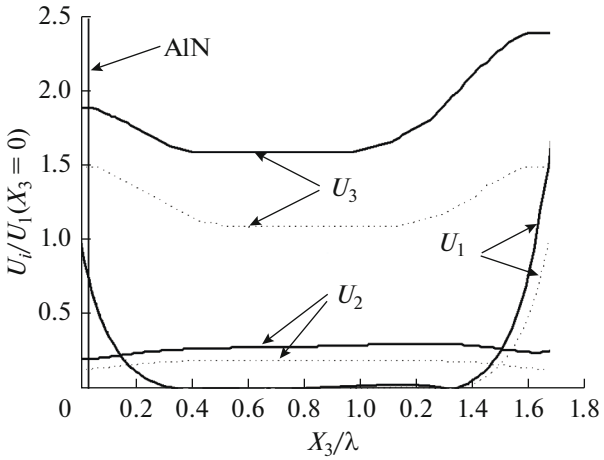

Fig. 4. The depth profiles of the first-order Lamb mode in uncoated ST,X-quartz plate (dotted) and the same plate coated with AlN film (solid). The thickness of the plate $H/\lambda = 1.67$. The thickness of the film $h_{AlN}/\lambda = 0.01$.

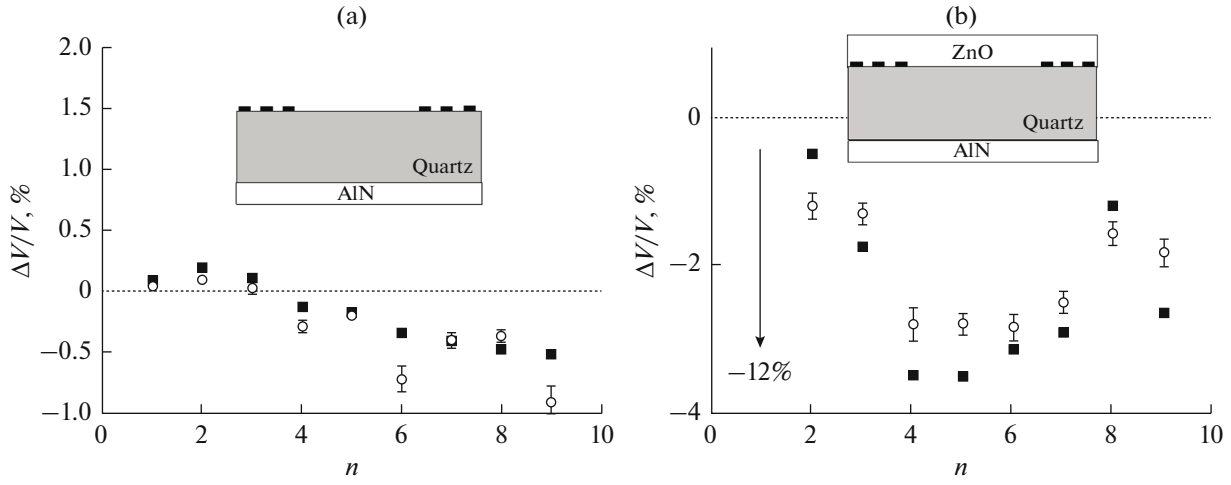

Fig. 5. Changes in the phase velocities of the SH-waves in ST,X + 90° plate produced by the films deposition as referred to the values in uncoated plate (● – calculations, ■ – measurements): (a) the plate ($H/\lambda = 1.67$) coated with AlN film ($h_{AlN}/\lambda = 0.01$); (b) the plate ($H/\lambda = 1.67$) sandwiched between AlN ($h_{AlN}/\lambda = 0.01$) and ZnO ($h_{ZnO}/\lambda = 0.0107$) films.

modes are decreased compared with uncoated quartz plate because of "small" velocity in ZnO. For $H/\lambda = 1.67$, $h_{AlN}/\lambda = 0.01$, and $h_{ZnO}/\lambda = 0.0107$ the reduction of the velocities is within −1...−12%.

Attenuation α of waves due to film deposition measured as the difference in delay line insertion loss for coated and uncoated plates is also different for various modes (Fig. 6). For example, for the 2nd SH-mode it is 0.5 dB/mm at 17.6 MHz, while for other modes it is 0.01–0.07 dB/mm at about same frequencies. The large values of the attenuation may be attributed to the textured structure of films making inter-atomic interaction between grains much weaker than inside them [16]. This property produces an increase in propagation loss and masks reduction of the transduction loss in transducers due to increased coupling constants (Fig. 3c).

Finally, Fig. 7 verifies asymmetry of mode profiles in the AlN/quartz structure predicted theoretically by Fig. 4. The figure shows the difference in mode attenuation Δα measured for the same loading (glycerin) deposited on the top and bottom faces. For uncoated plate (white), when the displacements of modes on both faces are equal to each other and the mode profiles are symmetric, the difference Δα is close to zero for all modes (precision of the measurements is ±0.5 dB). On the contrary, for the coated plate (gray) the difference Δα between attenuation on the top (uncoated) and bottom (coated) faces for most modes is much higher.

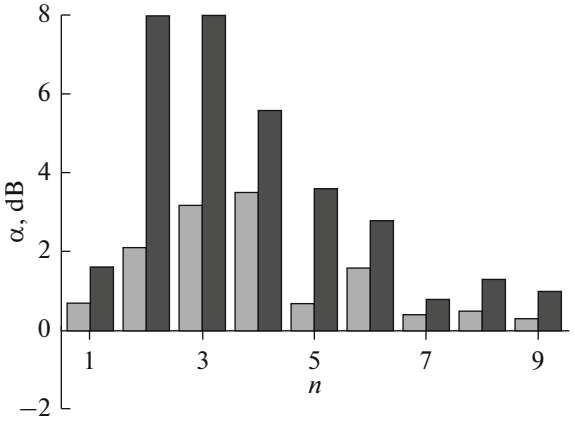

Fig. 6. Attenuation of the SH waves in ST,X+90° quartz plate produced by the films deposition as referred to uncoated plate. Gray – the plate ($H/\lambda = 1.67$) coated with AlN film ($h_{AlN}/\lambda = 0.01$). Black – the same plate sandwiched between AlN ($h_{AlN}/\lambda = 0.01$) and ZnO ($h_{ZnO}/\lambda = 0.0107$) films. The length of the acoustic path is $L = 16.5$ mm.

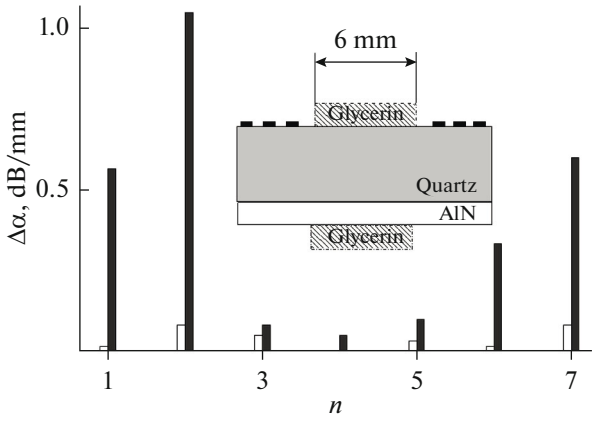

Fig. 7. Difference in the Lamb mode attenuation Δα produced by 6 mm long glycerin loading deposited on the top and bottom faces of the structure. White – uncoated ST,X-quartz plate ($H/\lambda = 1.67$). Dark gray – the same plate with AlN film ($h_{AlN}/\lambda = 0.01$) at the bottom.

Therefore, it may be concluded that in the AlN/quartz structure the top and bottom displacements of modes are not equal to each other, the modes profiles are no more symmetrical or anti-symmetrical, and the energy of modes is trapped to uncoated (top) face and repealed from the coated (bottom) counterpart.

4. CONCLUSIONS

The layered structures composed of a piezoelectric plate and piezoelectric films offer much larger variety of achievable acoustic characteristics as compared with uncoated plate of the same material. Proper selection of the films thickness, plate thickness, transducer configuration, mode order, and mode type allows increase or decrease of the phase velocities and coupling constants of modes. Classification of materials as "fast" and "slow" and piezoelectrically "strong" and "weak" usually used for Rayleigh waves in the layered structures is not valid for the waves propagating in the coated plates, in general.

The depth profiles of modes in layered plates are not symmetrical or anti-symmetrical.

Attenuation of modes due to imperfection of the film structure is remarkable.

ACKNOWLEDGMENTS

The work has been partially supported by Russian Science Foundation Grant no. 15-19-20046-P in frame of fabrication and testing the layered structures and by Russian Foundation of Basic Research Grant no. 17-07-00750 in frame of theoretical analysis of the structures. The development of layered waveguides for acoustic sensors was partially performed in the framework of the state assignment of Kotelnikov IRE RAS. The work was also partially supported by Russian Foundation for Basic Research, project no. 17-07-00750 in the framework of theoretical analysis of the structures.

REFERENCES

1. I. A. Viktorov, *Rayleigh and Lamb Waves-Physical Theory and Applications* (Plenum, New York, 1967).
2. B. A. Auld, *Acoustic Fields and Waves in Solids* (John Wiley and Sons, New York, 1973), **Vol. 1**, p. 423; **Vol. 2**, p. 414.
3. G. W. Farnell, in *Physical Acoustics—Principles and Methods,* Ed. by W. P. Mason and R. N. Thurston (Academic Press, New York, 1970), **Vol. 6**, p. 109.
4. A. M. Lomonosov, P. D. Pupyrev, and P. Hess, in *Proc. 2003 IEEE Ultrasonics Symposium* (Prague, July 21–25, 2003), p. 1362.
5. I. V. Anisimkin, Ultrasonics **42**, 1095 (2004).
6. V. I. Anisimkin, IEEE Trans. Ultrason., Ferroelectr. Freq. Control **57**, 2018 (2010).
7. F. Di Pietrantonio, M. Benetti, D. Cannata, R. Beccherelli, and E. Verona, IEEE Trans. Ultrason., Ferroelectr. Freq. Control **57**, 1175 (2010).
8. V. I. Anisimkin and N. V. Voronova, IEEE Trans. Ultrason., Ferroelectr. Freq. Control **58**, 578 (2011).
9. E. Verona, V. I. Anisimkin, V. A. Osipenko, and N. V. Voronova, Ultrasonics **76**, 227 (2017),
10. S. K. Tleukenov and A. B. Aitbaev, Acoust. Phys. **61** (2), 161 (2015).
11. Yu. M. Zaslavskii, Acoust. Phys. **62** (1), 87 (2015).
12. V. I. Anisimkin, Acoust. Phys. **62** (1), 1 (2015).
13. E. L. Adler, J. K. Slaboszewics, G. W. Farnell, and C. K. Jen, IEEE Trans. Ultrason., Ferroelectr. Freq. Control **37**, 215 (1990).
14. A. J. Slobodnik, Jr., E. D. Conway, and R. T. Delmonico, *Microwave Acoustic Handbook* (Air Force Cambridge Research Laboratories, Bedford, MA, 1973), AFCRLTR-73-0597.
15. G. W. Farnell and E. L. Adler, in *Physical Acoustics—Principles and Methods,* Ed. by W. P. Mason and R. N. Thurston (Academic Press, New York, 1972), **Vol. 7**, p. 35.
16. V. I. Anisimkin and I. M. Kotelyanskii, Russ. Phys.: Solid State Phys. **30**, 853 (1988).